

VELOCITY AND TOTAL PRESSURE MEASUREMENT IN THE TWO-STAGE HYBRID THRUSTER TIHTUS

H. Böhrk, M. Auweter-Kurtz

Institut für Raumfahrtssysteme (IRS), Universität Stuttgart,
Pfaffenwaldring 31, D-70550 Stuttgart, Germany

boehrk@irs.uni-stuttgart.de

Abstract

A novel hybrid two-stage electric thruster (TIHTUS) is under development at IRS. It provides the possibility to supply power and mass-flow through either stage into the plasma. A variation of power- and mass-flow-staging was investigated with a Pitot probe and an electric time-of-flight probe. The present paper discloses the radially resolved measurement results of total pressure and plasma velocity at a downstream position of 200 mm. Furthermore, a method is presented to access radially resolved flow temperature from the combined pressure and velocity measurement. The temperature data are also presented. For a sum of powers of 50 kW at 300 mg/s, the Pitot pressure maximum is at 85 Pa while maximum velocity is measured as 9224 m/s and 10350 m/s for two respective conditions.

Thruster Concept

The current limitations to the exhaust velocity of hydrogen previously heated in a plenum of a rocket engine are imposed due to various reasons. At low stagnation pressures, the high bulk enthalpy added, although high, is largely transformed into dissociation and ionisation but cannot be directed to kinetic energy when expanded to lower pressures in a nozzle. Or the bulk enthalpy is, although useful, low at high stagnation pressures. Or, finally, the enthalpy that, at optimum pressure, can be converted to directed kinetic energy shows a maximum but is a compromise between the two features mentioned above [1]. When both, gas temperature and stagnation pressure, are increased, the optimum will collide with limitations due to the electrode material. Therefore, new thruster concepts are required in order to produce relatively high exhaust velocity at relatively high thrust.

Exhaust velocity c_e of any thermal thruster is dependent on the propellant temperature T_0 in the combustion cham-

ber and its molecular mass M according to

$$c_e \propto \sqrt{\frac{T_0}{M}}. \quad (1)$$

The average propellant temperature should, therefore, be as high as possible. Currently, the highest exhaust velocities of thermal propulsion concepts that use stationarily chamber heated, hydrogen range between 20 und 25 km/s [2].

Arcjet thrusters have been developed throughout the past decades. They provide relatively high thrust at moderate exhaust velocities. An arcjet thruster has a central cathode and an annular anode. The propellant is injected into the ring-shaped gap between the two electrodes and heated up by an electric arc. It is then expanded and accelerated through a nozzle where the energy contained in the plasma is transferred to directed energy. The plasma flow of a thermal arcjet is characterized by high specific enthalpy and high flow velocity. These characteristics are, however, combined with the presence of steep radial property gradients as in a hot, energy-rich core with a relatively cold gas layer at its edge.

An idea to transfer more power into the plasma flow is to reheat these edges of the plume by a second heating mechanism in the way of an afterburner. The principle is sketched in *figure 1*. TIHTUS (Thermal-inductive hybrid thruster of the Universität Stuttgart) is a two-stage plasma generator where reheating is realized by means of inductive heating. This new concept has the potential of producing large thrust and high effective exhaust velocity by addition of power in the second stage [3]. It is therefore considered the predecessor of a future propulsion system for the transport of heavy payload on interplanetary trajectories [4, 5].

TIHTUS consists of an arcjet thruster (first stage) and an inductively heating afterburner (second stage). The second stage consists of a discharge tube and a coil spun around it

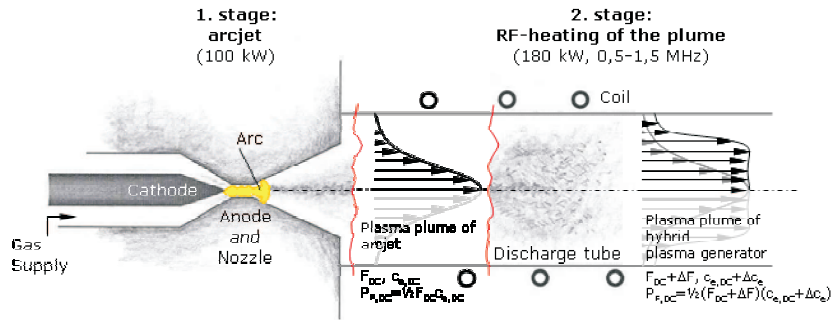


Figure 1 Principle of TIHTUS

being part of a resonance circuit. The inductively heated plasma generator (IPG) is used as the afterburner since in induction heating, due to the skin-effect, the power is coupled into the plasma at near-coil position, where the cold gas layer of the arcjet plume is located [6]. The plasma jet emerging from the arcjet is thus expanded into the quartz discharge tube. The alternating RF-current in the coil induces an oscillating, mostly azimuthal, magnetic field inside the tube. This field initiates an electric discharge in the propellant oriented in the opposite direction of the coil current. The free electrons contained in the plasma from the thermal arcjet are accelerated by the electric field and by means of collisions they transfer their induced power to the atoms and molecules. RF-power is thus coupled into the plasma.

It has been shown that with the currently used set-up, two-stage operation of the thruster is possible [3, 4]. The principal question is whether it is possible to specifically heat the outer edges of an arcjet plume so that higher exhaust velocity can be attained. Of course, a dependency of power to each stage is expected as well a dependency of the gas mass flow rate is evident.

The thruster is operated as a water-cooled model using hydrogen as propellant. Power may be coupled into the arc heated (DC) or the inductively heated (RF) stage. Gas flow through the arc heated stage is expanded first into the injection head of the inductive, second, stage where a swirl gas flow can be admixed. The operational condition is therefore declared as $T P_{DC} | P_{RF} - \dot{m}_{DC} | \dot{m}_{RF}$ throughout this paper. The investigated conditions are listed in *table 1*.

Table 1 Nomenclature for operational condition.

	P_{DC} [kW]	P_{RF} [kW]	\dot{m}_{DC} [mg/s]	\dot{m}_{swirl} [mg/s]
T 50 00-300 0	50	0	300	0
T 25 25-300 0	25	25	300	0
T 20 30-300 0	20	30	300	0
T 25 25-200 100	25	25	200	100
T 25 25-100 200	325	25	100	200

The radial profiles of total pressure and plasma flow velocity are measured by means of a Pitot probe and a time-of-flight electric probe, respectively. As mentioned above, the propellant temperature is of main interest. However,

high temperature is a very delicate state variable and difficult to measure. In the present work, using the measured data of velocity and Pitot pressure, a new method will be presented to deduce temperature information.

After having introduced the thruster principle above, the present paper will present the setup of the ground test facility and the probe setup of Pitot and time-of-flight probes. Furthermore, the methodology is introduced, by means of which temperature information is derived from Pitot pressure and velocity. In the results section, radial profiles of total pressure and velocity are shown for the listed operating conditions and interpreted. Last, radial temperature profiles are presented and conclusions are drawn choosing the preferable operating point.

Experimental Apparatus

The TIHTUS ground test facility consists of the two plasma sources and the vacuum chamber. TIHTUS' first stage is HIPARC-W(water-cooled) and foreseen for up to 100-kW-operation. It is supplied by a 6-MW-DC-power supply. The second stage is an IRS-IPG configuration with 3.5 coil windings and four capacitors, resulting in a nominal operational frequency of 840 kHz. The device is connected to a 180-kW radio-frequency power supply able to be operated at frequencies ranging from 0.5 to 1.5 MHz. The scheme of the facility is depicted in *figure 2*. Installed are a gas supply system, water-cooling system and a data acquisition system. The size of the vacuum chamber is about 2.5 m in length and 2 m in diameter. Its lid carries the thruster and the external resonance circuit. The rear end of the chamber is connected to the IRS vacuum pump system, the total suction power of which amounts to 6000 m³/h at atmospheric pressure or 250 000 m³/h at 10 Pa.

Both parts of the thruster are water-cooled at present. Therefore, coolant flow rates are measured as are the flow rates of the propellant. However, at a further stage of development, the strategy foresees building the plasma source in a radiation-cooled design, which promises another gain in specific impulse.

For plume investigation, a two-axes table is installed inside the vacuum tank on which probes can be mounted.

Pitot Probe

The total, or Pitot, pressure is the pressure present in the foremost stagnation point of a body inserted into a

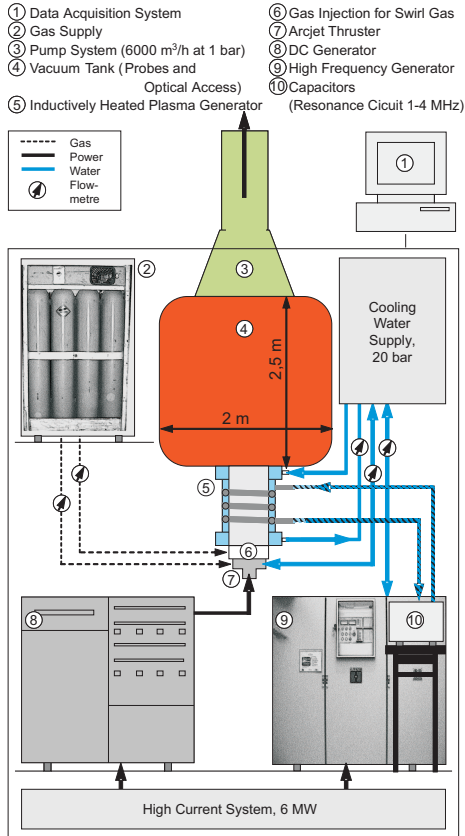


Figure 2 Scheme of the experimental apparatus

plasma column, such as a Pitot probe. Within the probe the deceleration of the flow takes place isentropically. The pressure measured at the end of a Pitot tube, therefore, corresponds to the total pressure in the stagnation point in front of the tube opening. At $Ma \geq 1$, this is the plenum pressure just behind an imaginary vertical, ideal bow shock. In a supersonic flow, the Pitot probe, therefore, does not measure the total pressure in the free stream. The ratio of the true total pressure of the free stream to the measured total pressure behind a bow shock is [7]

$$\frac{p_{tot,1}}{p_{tot,2}} = \left(\frac{2\kappa}{\kappa+1} Ma^2 - \frac{\kappa-1}{\kappa+1} \right)^{\frac{1}{\kappa-1}} \left(\frac{1 + \frac{\kappa-1}{2} Ma^2}{\frac{\kappa+1}{2} Ma^2} \right)^{\frac{\kappa}{\kappa-1}}. \quad (2)$$



Figure 3 Pitot probe.

The Pitot probe used in the present case is of European standard geometry (flat nose, 50 mm body diameter, rounded edge) with a measurement orifice of 26 mm diameter. It is depicted in *figure 3*. For proof of reproducibility, the measurement points were detected twice and averaged values are presented here.

Electric Time-of-Flight Probe

For the measurement of the plasma velocity v_∞ , electric time-of-flight probes are applied. Electric probes are electrically conductive measurement devices exposed to a plasma. A double probe has two electrodes with a voltage applied between them. Due to an electrically conductive plasma passing between the electrodes, a current can be measured. The measurement principle for plasma velocity is based on the axial offset of two double probes. The current flow between either pair shows fluctuations in the plasma which translate with plasma velocity from the first to the second double probe. The principle is depicted in *figure 4*. The electrodes are of tungsten wire with a diameter of 0.5 mm and the two double probes have an axial offset of 26 mm. An example of the probe signals are shown in *figure 5*. At each radial position 5 pairs of curves were

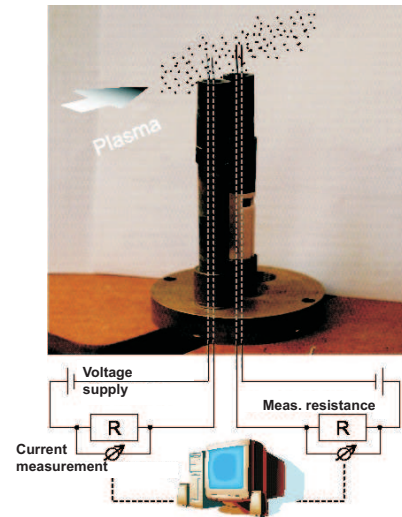


Figure 4 Electric time-of-flight probe setup.

recorded. The velocities determined from their correlation were then averaged.

The voltage induced into the electrodes by the RF magnetic field is dependent upon the magnetic field strength B and the projected area A_{proj} of the electrodes according to

$$V_{ind} = \dot{B}A_{proj} + B\dot{A}_{proj}. \quad (3)$$

Consequently, the probes are arranged so that all four cylindrical probes of the two double probes are axially aligned with the plume axis so that the projected area is minimized.

Methodology

In the present elaboration, the plume of two-staged TIHTUS thruster is investigated by a Pitot pressure and an electric time-of-flight probe. A novel method is introduced, here, in which from total pressure and velocity, temperature is deduced.

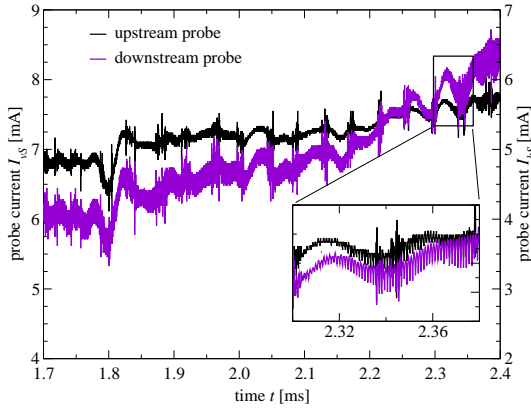


Figure 5 Probe data from operational condition T 25|25-100|200.

Mach number is defined as

$$Ma = \frac{v}{a} = \frac{v}{\sqrt{\kappa RT}} \quad (4)$$

with the speed of sound a , the isentropic exponent κ , and the specific gas constant R . Depending on Mach number, in the stagnation point a total pressure is formed so that

$$\frac{p_{tot}}{p_{\infty}} = \left(\frac{\kappa + 1}{2} Ma^2 \right)^{\frac{\kappa}{\kappa - 1}} \left(2 \frac{\kappa}{\kappa + 1} Ma^2 - \frac{\kappa - 1}{\kappa + 1} \right)^{\frac{1}{1 - \kappa}} \quad (5)$$

in supersonic and

$$\frac{p_{tot}}{p_{\infty}} = \left(1 + \frac{\kappa - 1}{2} Ma^2 \right) \frac{\kappa}{\kappa - 1}. \quad (6)$$

in subsonic flow [8]. The isentropic exponent κ is a function of temperature. It was shown by Laure, that a deviation has only little influence on the result of Mach number from eq. (5) [9]. The data presented here are furthermore based on the assumption that the ambient pressure in the vacuum tank is imposed on the plasma plume. This assumption is also supported by Refs. [10] and [11].

Just like the isentropic exponent κ , the specific gas constant R is dependent of temperature. In the present study, their value was taken from Ref. [12] and is based on a plasma composition model assuming thermodynamic equilibrium. Transferring eq. (4) to a function for velocity v of temperature T results in

$$v^2 = Ma^2 \kappa(T) R(T) T. \quad (7)$$

Figure 6 shows the velocity of a plasma plume as derived from eq. (7) for a total pressure ratio measured at T 50|00-300|0.

For the same operating point and position, the velocity measured by electric probes is marked in the graph as a horizontal line. In the figure, the velocity derived from Pitot probe measurement for a variety of temperatures and the velocity measured with electric probe intersect. Namely, at the temperature for the pressure ratio of which the “true” velocity was measured by the electric probes. This temperature is the plasma temperature at the position and the operating position. This means that the local temperature is derived from velocity and total pressure measurements

while only two assumptions have to be made: a perpendicular, ideal bow shock in front of the Pitot probe and plasma fluctuations measured by the electric probes moving with plasma velocity. Furthermore, isentropic exponent and specific gas constant were calculated from a model considering thermo-chemical equilibrium [12].

In the framework of the present measurement campaign, a radial profile of plasma velocity was measured for the five operating conditions of table 1. Hence, for each point of measurement in each radial profile the temperature is determined from Pitot probe and electric time-of-flight measurements

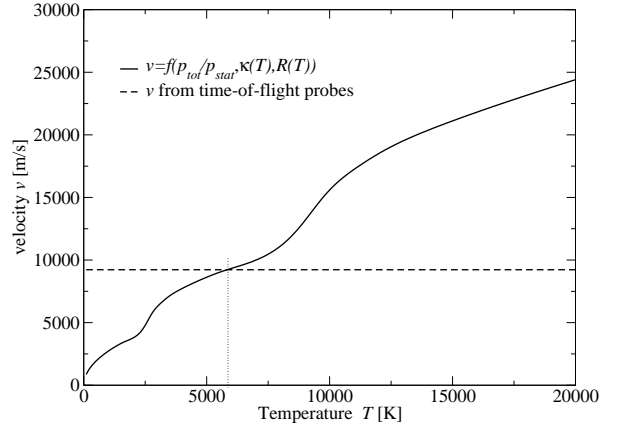


Figure 6 Scheme of temperature determination method.

Results and Interpretation

As was described in the introduction, in TIHTUS, electric power can be applied to either the arc heated stage, the inductively heated stage, or to both stages. Also, the ratio of the gas flows through either stage can be varied. The five operating conditions of table 1 were investigated. They include a variation of power staging for a gas flow relation of 300|0 mg/s and a variation of mass flow staging for constant power staging of 25|25 kW.

The radial profiles of total pressure and plasma flow velocity are measured by means of a Pitot probe and a time-of-flight electric probe, respectively. As mentioned, propellant temperature is of main interest and thus, a new method will be presented to obtain a radial temperature profile from velocity and total pressure.

Radial profiles were investigated at an axial position of $x=200$ mm from the thruster exit.

Pitot Pressure

Figure 7 shows Pitot pressure in the plane perpendicular to the plume exhaust direction with a mass flow rate of 300 mg/s through the arcjet thruster stage. The maxima at eccentric position originate from the plasma flow through the discharge tube instead of a diverging nozzle. The curve marked with hollow triangles represents only arc heated stage active at 20 kW. It shows maxima at eccentric position, while the plume is quite narrow. Black triangles mark the same arcjet power with second stage power added to it. It becomes evident, that the power of the inductively heated stage is coupled into the plasma annularly at eccentric position. for reasons of clarity in the figure, error bars

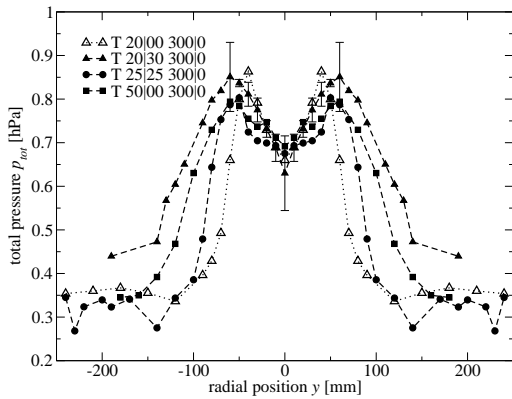


Figure 7 Pitot pressure at variation of power partitioning.

are marked only in the curve for T 20|30-300|0. They originate from the standard deviation of the measurements plus the pressure gauge error.

The black symbols represent conditions with power staging adding up to 50 kW each. At the plume center, it can be observed that higher total pressure is produced with increasing arc power. The highest maxima representing a total pressure of 0.85 Pa are achieved with 20 kW supplied from the arc heating stage and 30 kW coupled into the plume by inductive heating. The same condition shows the widest plume diameter. This can be interpreted as the most power coupled into the plasma at coil-near position. However, the smallest diameter is *not* reached at pure arc heating with 50 kW but with 25 kW arc and 25 kW inductive heating.

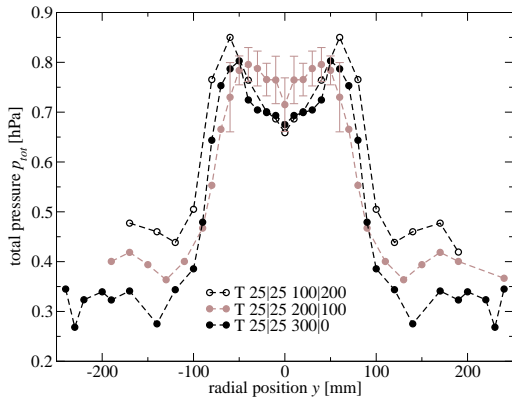


Figure 8 Pitot pressure at variation of mass flow rate partitioning.

For a power staging of 25|25 kW, a gas flow variation was conducted. The Pitot pressure graphs are presented in *figure 8*. From the edges of the plume, it can be seen that according to the measurement condition and the mass flow staging, the ambient pressure in the tank varies between 0.34 and 0.4 Pa. In the second stage, the gas flow is injected radially as swirl gas. It is observed that the more gas is injected as swirl gas, the higher the ambient pressure. The diameter of the plasma plume, however, does not remarkably change with varying mass flow staging. Total pressure maxima of 0.85 Pa are reached for 100|200 mg/s.

From these measurements, the highest integral of total pressure is reached with T 20|30-300|0. The data have been compared to thrust measurements in Ref. [13].

Velocity

In *figures 9* and *10*, plasma velocities investigated with electric time-of-flight probes are depicted. Please note that measurements could only be taken in the plume center, where ionization of the plasma was high enough to have a current flow through the plasma and the electric probes. Profiles were able to be recorded out to a radial distance of 150 mm from the plume center.

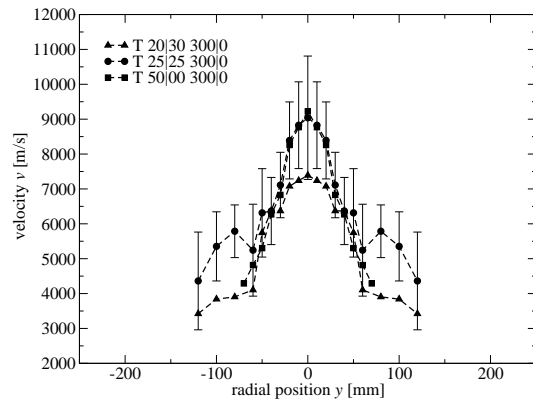


Figure 9 Velocity at variation of power partitioning.

Figure 9 represents the variation of power staging according to the pressure data presented above. The curves do not have the excentric maximum shape as the Pitot pressure curves. They demonstrate a maximum at centric position. The center values, as according to the Pitot center values, increase with increasing first stage power. Power partitioning of 25|25 reaches almost the maximum velocity of 9224 m/s in the plume center that were reached by the one of 50|0 with an addition of power at the plume edge. Of much smaller amount is the maximum of the power staging with 20|30 kW. This means that when too little power is applied by the first stage, ionization is not high enough for the induction coil to efficiently couple power into the plasma. Furthermore, velocity decreases while the profile gains in diameter.

At maintained power ratio of 25|25 kW, the gas flow variation shows that with pure flow through the arcjet, a maximum is formed in the plume center. However, for increasing swirl gas flow, the maxima become excentric. This is most extreme for 100 mg/s of hydrogen fed through the arcjet and 200 mg/s fed through the injection head. The highest local velocities of >10,300 m/s are reached with 200 mg/s of hydrogen fed through the arcjet and 100 mg/s fed through the injection head. The plume centers show an increase in velocity with increasing arcjet flow.

For a thruster, the exhaust velocity should be high. This is meant with respect to the integral exhaust velocity. Among the investigated conditions, the integral is maximized for T 25|25-300|0.

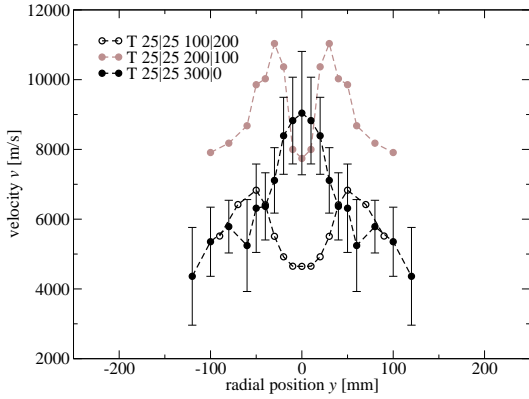


Figure 10 Velocity at variation of mass flow rate partitioning.

Temperature

By means of the method described above, the temperature is derived from Pitot pressure and plasma velocity. The isentropic coefficient used was from Ref [12] providing data depending on temperature and static pressure.

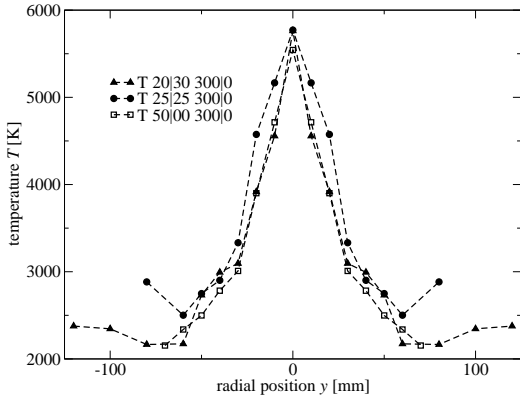


Figure 11 Temperature at variation of power partitioning.

It becomes evident from *figure 11* that for all operating conditions using pure central gas flow at 300 mg/s the temperature profile is very similar at any power staging. This indicates that the thermal efficiency of the coupling of the inductive, second, stage into the plasma is high. Equation (7), shows that temperature is quadratically proportional to velocity but anti-proportional to $\left(\frac{p_{tot}}{p_{stat}}\right)^{f(\kappa)}$. The isentropic exponent lies between 1 and 1.67 and can thus be seen that for high total pressure the temperature must be low while for high velocity the temperature is high. *Figures 7* and *9* show that Pitot pressure has excentric maxima while velocity does not. Therefore, at increasing distance from the center, the temperature shows steep temperature gradients, since velocity falls and total pressure rises.

The widest temperature profile is the one for T 25|25 300|0, which shows the narrowest Pitot pressure profile. The profile of T 20|30 300|0 follows closely that of T 50|00 300|0 although velocity was comparatively low, since also Pitot pressure is low, especially in the plume

center. Pitot pressure then increases steeply while velocity shows a rather shallow profile.

For the variation of mass flow rate staging, depicted in *figure 12*, it is found that, according to the behaviour of the velocity, with increasing swirl gas flow, the maxima become excentric and diverge. However, with pure arc heated flow, expanded through the arcjet nozzle and next through the discharge tube, there is a temperature maximum in the plume center. It was expected for the flow to have increasing temperature in the plume center for decreasing central gas flow. Still, the measurements show decreasing temperature in the plume for increasing swirl gas flow. This indicates that the cold swirl gas mixes with the central gas. This is possible since by means of the discharge tube of the second stage, the plume cannot unfold as it would but is forced against the cooled injection head where additionally a cold gas stream is injected.

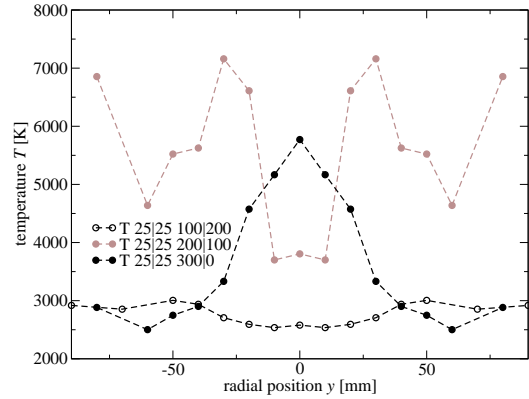


Figure 12 Temperature at variation of mass flow rate partitioning.

Equation (1) had shown that maximum effective exhaust velocity can be reached with the hottest plasma. The plasma with the maximum integral temperature is generated with T 25|25-300|0, producing the widest plume, although still, steep gradients are present in the plume.

Conclusions

The two-staged, hybrid thermal thruster TIHTUS can be operated in purely arc heated, purely inductively heated, or combined operation. It can be stationarily operated with a power of 50 kW.

Pitot pressure and plasma velocity were measured in a radially resolved manner at an axial downstream position of $x=200$ mm from the exhaust plane. Total pressure maximum is at 85 Pa while maximum velocity is measured at 9224 m/s for T 50|00-300|0 and 10350 m/s for T 25|25-200|100. The Pressure profile is mostly in “M”-shape indicating that the plume is a turbulent freejet. Velocity profile shape is dependent on gas-flow staging. The maxima move to excentric positions with increasing swirl gas injected.

From both, pressure and velocity profiles, it is shown that power coupling of the second stage takes place in the typical off-axis position close to the discharge coil.

A new method is introduced to determine radially resolved temperature from the total pressure and velocity profiles. The plasma temperature maxima measured are

5772 K and 7159 K for T 50|00-300|0 and T 25|25-200|100, respectively. Large temperature and velocity are detected at T 25|25-200|100, making them the favoured operating condition for high plasma velocity while for high total pressure T 20|30-300|0 provides the highest integral Pitot pressure.

The pitot pressure measurements are compared to thrust measurement in Ref. [13].

Acknowledgement

The Authors would like to thank Dr. Thomas Stöckle for initiating the idea of temperature deduction, Dr. Stefan Löhle for fruitful discussions and their students Melanie Lücke und Markus Mayer for their contribution to the presented experiments.

References

- ¹ BONNEVILLE, J.M., "High-Frequency Supersonic Heating of Hydrogen for Propulsion," AIAA Electric Propulsion Conference, Colorado Springs, CO, Mär. 1963.
- ² WALLNER, L.E., CZIKA, J., "Arc-Jet Thrustor for Space Propulsion," Tech. rep., NASA, Lewis Research Center, Cleveland, OH, 1965.
- ³ BÖHRK, H., AUWETER-KURTZ, M., "Preliminary Results of TIHTUS Operation," AIAA 2007-5158, Sacramento, CA, Jul. 2006.
- ⁴ BÖHRK, H., SCHMIT, T., AUWETER-KURTZ, M., "Flexible Piloted Mars Missions using the TIHTUS Engine," Aerospace Science and Technology, 2006, accepted.
- ⁵ BÖHRK, H., LAURE, S., AUWETER-KURTZ, M., "Feasibility Study of Application of ATTILA to In-Space Propulsion for Piloted Missions," IAC-04-S.4.03, Vancouver, Kanada, Okt. 2004.
- ⁶ ECKERT, H.U., "The Induction Arc: A State-of-the-Art Review," Journal of High Temperature Science, Vol. Vol. 6, 1973, pp. 99–134.
- ⁷ FROHN, A., Einführung in die Technische Thermodynamik, AULA-Verlag, Wiesbaden, 2nd ed., 1989.
- ⁸ LIEPMANN, H.W., Roshko, A., Elements of Gasdynamics, John Wiley and Sons, Inc., New York-London, 3rd ed., 1960.
- ⁹ LAURE, S., Experimentelle Simulation der Staupunktströmung wiedereintretender Raumflugkörper und deren Charakterisierung mittels mechanischer Sonden, Dissertation, Universität Stuttgart, Fak. Luft- und Raumfahrttechnik, 1998.
- ¹⁰ LAURE, S., AUWETER-KURTZ, M. FASOULAS, S., HABIGER, H., SCHÖNEMANN, A., "Experimentelle Simulation einer hochenthalpen Luftströmung im Plasmawindkanal," Jahrbuch der deutschen Gesellschaft für Luft- und Raumfahrt, Vol. 3, DGLR, Erlangen, 1994.
- ¹¹ ABRAMOVICH, G.N., Theory of Turbulent Jets, MIT Press, 1963, p269.
- ¹² PATCH, R.W., "Thermodynamic Properties and theoretical Rocket Performance of Hydrogen to 100,000 K and $1.01325 \times 10^8 \text{ N/m}^2$," Tech. rep., NASA, Lewis Research Center, Cleveland, 1971.
- ¹³ BÖHRK, H., AUWETER-KURTZ, M., "TIHTUS Thrust Measurement with a Baffle Plate," AIAA 2007-5297, Cincinnati, OH, Jul. 2007.



A revised version of this article is available here.